Coherent spectroscopy of a strongly driven triple quantum dot molecule*

Xie Yan(解 研), Duan Su-Qing(段素青),
Chu Wei-Dong(楚卫东)†, and Yang Ning(杨 宁)

Institute of Applied Physics and Computational Mathematics, Beijing 100088, *China*

(Received 8 April 2010; revised manuscript received 17 June 2010)

Based on a calculation model, we study the interference phenomena of serially coupled V-type and Λ-type triple quantum dots (CTQDs) driven simultaneously by a strong driving field and a weak probe field. Strongly depending on the configuration of the three-level CTQD, the probe absorption spectra, which are shown in the tunneling current, exhibit various quantum coherence properties. In the case where the two pairs of transitions of the CTQD have a small eigenfrequency difference $\Delta\omega$, the double-coupling effect of the driving field results in two Autler–Townes doublets and one weak Mollow triplet in one spectrum. With the value of $\Delta\omega$ increasing, only one Autler–Townes splitting remains due to the single-coupling of the field. We also find that the effect of spontaneous emission of phonons may lead to an obvious background current, which can be used to distinguish which transition is driven by the driving field in experiment. The interesting quantum property of a CTQD revealed in our results suggests its potential applications in quantum modulators and quantum logic devices.

Keywords: coherent spectroscopy, coupled quantum dots, quantum transport, photon assistance
PACC: 7320D, 0560

1. Introduction

Recently, coupled triple quantum dots (CTQDs) have attracted much attention. Due to the various electronic structures and the flexible tunabilities of CTQDs beyond those of a single or double quantum dots (QDs), unique quantum properties have been discovered theoretically and experimentally in CTQDs, for example, tunneling transport,[1−3] Fano coherence,[4−6] Kondo effect,[7,8] spin coherent states[9−11] and so on. Besides these physical phenomena, photon-assisted transport and optical interference are also worth investigating in CTQDs.

Quantum interferences based on three-level systems are well studied in atom optics, where the typical quantum coherence effects include coherent trapping and electromagnetically induced transparency. As artificial atoms and molecules, single and coupled QDs have similar quantum coherent behaviours[12−14] which can be exhibited in the optical and the electrical transport phenomena of the system. Recently, interesting interference spectra related to three-level quantum systems are observed in a single semiconductor QD driven by two optical fields.[15] In fact, an adjustable three-level configuration can be more easily formed in a CTQD. In experiments,[2,3] the electronic structure of each dot of a CTQD is controlled independently by using plunger gates, and the controllable factors also include the coupling between dots. An optical coupling three-level system can be formed by taking one level from each dot and be designed as a V-, or Λ-, or Ξ- type configuration by engineering the dot levels. On the other hand, the detection of quantum behaviour of a CTQD has been carried out through electrical transport signals in experiment. Therefore, a CTQD provides an appropriate platform for the study of the quantum interference based on a three-level system.

In this paper, the quantum interference in a serially CTQD driven simultaneously by a strong field and a weak field is studied by calculating the photon-assisted tunneling current through the system. Each dot of the CTQD provides one state and a hybridised three-level system is formed through the coupling between middle and left (right) dots (see Figs. 1(b) and 1(c)). In such a system, two pairs of transitions, $|0\rangle \rightarrow |1\rangle$ and $|0\rangle \rightarrow |2\rangle$, are allowable to be driven by both of the optical fields. The optical coupling affects the population of electrons in the levels, which can manifest itself in the tunneling current of the CTQD. Spontaneous emission of phonons, which also influ-

*Project supported by the National Natural Science Foundation of China (Grant No. 10774016).
†Corresponding author. E-mail: chu_weidong@iapcm.ac.cn
© 2010 Chinese Physical Society and IOP Publishing Ltd

ences the electron population and induces a characteristic background current, is investigated as well. Rich quantum interference phenomena are found in photon-assisted current spectra of CTQDs as the energy difference between E_1 and E_2 is small, at which the strong field can drive two pairs of transitions, simultaneously. The underlying physics of the quantum interference is revealed in a dressed-electron picture.

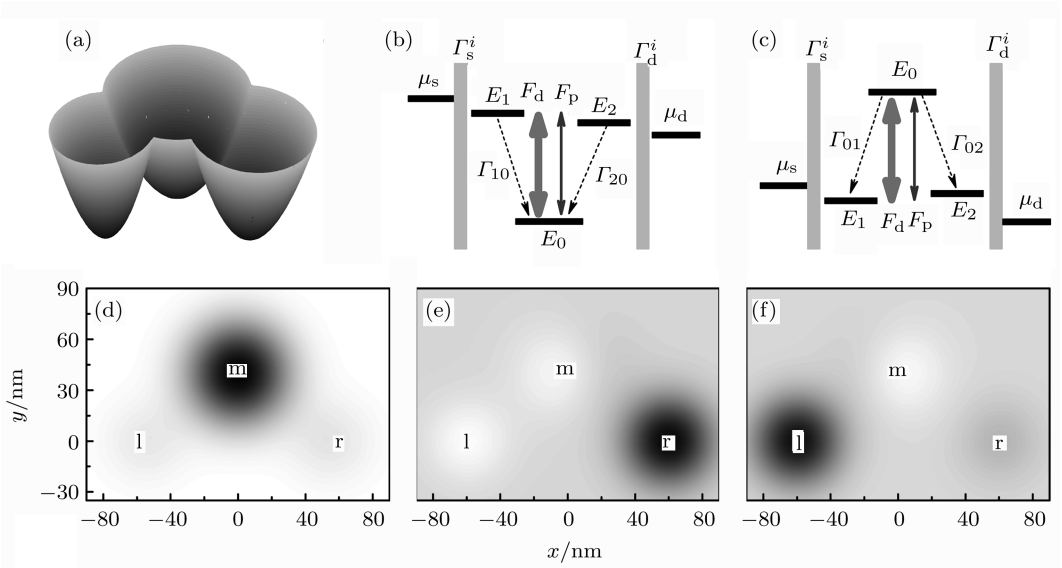


Fig. 1. Potential model for a CTQD (a). Level schemes for a V-type (b) and Λ-type (c) CTQD driven by a strong driving field F_d and a weak probe field F_p. (d)–(f) Wave functions of the ground state (d), the first (e) and the second (f) excited states of a V-type CTQD, respectively. Centres of the dots are marked by l, m and r, respectively. The potential parameters are $\hbar\omega_l = 5.5$ meV, $\hbar\omega_m = 4.0$ meV, and $\hbar\omega_r = 5.3$ meV.

2. Model and calculation

2.1. Hamiltonian and equations of motion

We study the quantum coherence spectroscopy of a strongly driven CTQD by calculating the two-mode photon-assisted tunneling current of the CTQD. We start our study by calculating the electronic eigenstates of the CTQD. According to recent experiments[2,3] on the charging diagram and tunneling conductance of CTQDs, we choose our model to follow the energy and length scales of real CTQDs. Under the effective mass approximation, the Hamiltonian of an electron in CTQD is written as

$$H_0 = \frac{\boldsymbol{p}^2}{2m^*} + V(x,y), \tag{1}$$

with m^* being the effective mass of electron. We adopt a parabolic model to describe the confining potential of a dot. And then the whole potential of the CTQD can be written as

$$V(x,y) = \frac{1}{2}m^* \min\{\omega_l^2[(x-x_l)^2+y^2], \omega_m^2[(x-x_m)^2+(y-y_m)^2], \omega_r^2[(x-x_r)^2+y^2]\}, \tag{2}$$

where $(x_l, 0)$, (x_m, y_m) and $(x_r, 0)$ are position coordinates of the left, middle and right dots, respectively, and ω_l, ω_m and ω_r are confining frequencies of the QDs. The confining potential is given in Fig. 1(a). Using electron states of the three single dots $|\Phi_j^k\rangle$ (j = m, l, r) to construct a nonorthogonal basis, one can obtain the eigenstates of the CTQD by solving a general eigenvalue problem, i.e., $|i\rangle = \sum_k c_{il}^k|\Phi_l^k\rangle + c_{im}^k|\Phi_m^k\rangle + c_{ir}^k|\Phi_r^k\rangle$. In our calculation, we adopt the parameter of GaAs material as $m^* = 0.067m_e$. In Figs. 1(d)–1(f), we plot the wave functions of the three lowest states $|i\rangle$ ($i = 0, 1, 2$) in the potential with $\hbar\omega_l = 5.5$ meV, $\hbar\omega_m = 4.0$ meV, and $\hbar\omega_r = 5.3$ meV. It is clear that the electron wave extends beyond one dot due to the tunneling between dots, which means that the state is hybridised. The energies of the three states are $E_0 = 3.99$ meV, $E_1 = 5.29$ meV and $E_2 = 5.49$ meV, which form a V-type level configuration as shown in Fig. 1(b). The level configuration can be changed by varying the dot potentials and positions, and another level configuration can also be obtained, for example, a Λ-type one as depicted in Fig. 1(c).

The tunneling between a CTQD and its electron reservoirs can be controlled by applying electric voltages to gate electrodes in experiment. Theoretically, such tunneling effects are described by the tunneling rates $\Gamma_{\rm s}$ between dot and source and $\Gamma_{\rm d}$ between dot and drain. In our discussion, the tunneling coupling between the CTQD and the electron reservoirs is weak, and then the wide-band limit[16,17] is used, where $\Gamma_{\rm s}$ and $\Gamma_{\rm d}$ are taken to be constant. For the hybridised state $|i\rangle$, the incoming and the outgoing tunneling rates through it are $\Gamma_{\rm s}^i = \sum_k |c_{il}^k|^2 \Gamma_{\rm s}$ and $\Gamma_{\rm d}^i = \sum_k |c_{ir}^k|^2 \Gamma_{\rm d}$, respectively.

For our studied V-type and Λ-type three-level CTQDs, the photon assistance strongly affects the electron transport behaviour. In the wide-band limit, the photon assistance mainly happens through the inter-dot barriers, and that through the barriers between the dots and the reservoirs can be neglected.[18] We consider two linearly polarised fields applied to the CTQD, simultaneously: one is strong and acts as a driving field $F_{\rm d}$, the other is weak and serves as a probing field $F_{\rm p}$. Due to the fact that the scale of electron movement is far smaller than the wavelength of the fields, the electron-field interaction can be considered in the dipole approximation. The dipole matrix element between $|i\rangle$ and $|j\rangle$, which depends on both the field polarisation direction $\boldsymbol{e}$ and the inter-dot coupling, is written as $d_{ij} = e\langle i|\boldsymbol{e}\cdot\boldsymbol{r}|j\rangle$ with e being the elementary charge. For the V- and the Λ-type CTQDs shown in Figs. 1(b) and 1(c), we are mainly interested in the quantum coherence phenomena caused by the optical couplings between $|0\rangle$ and $|1\rangle$ and between $|0\rangle$ and $|2\rangle$. This requires that both d_{01} and d_{02} should be much larger than d_{13}, which can be realized by tuning the direction of $\boldsymbol{e}$ and the dot positions of the CTQD. For the model CTQD shown in Fig. 1, $\boldsymbol{e}$ is placed along the y direction, and $d_{01} = 0.09$, $d_{02} = 0.1$ and $d_{12} = 0.0006$ (arbitrary unit) are obtained for the energy interval $S = E_2 - E_1 = -0.2$ meV. Close values of d_{01}, d_{02} and d_{12} can be also obtained for CTQDs with different values of S. For simplicity, we fix d_{01} and d_{02} at the same value and take $d_{12} = 0$ but vary S to investigate different CTQDs.

We consider the quantum interference in the near-resonant condition, where the detuning $\Delta_{\rm d(p)}^j$ of field $F_{\rm d}$ ($F_{\rm p}$) satisfies $\Delta_{\rm d(p)}^j \ll \hbar\omega_{0j} + \hbar\omega_{\rm d(p)}$ with $\hbar\omega_{0j} = |E_j - E_0|$ and $\hbar\omega_{\rm d(p)}$ being the field frequency ($j = 1, 2$). In this case, the rotating-wave approximation is valid and the interaction Hamiltonian is written as

$$H_{\rm I} = \hbar\Omega_{\rm d}^1 a_1^\dagger a_0 {\rm e}^{{\rm i}\Delta_{\rm d}^1 t} + \hbar\Omega_{\rm d}^2 a_2^\dagger a_0 {\rm e}^{{\rm i}\Delta_{\rm d}^2 t} + \hbar\Omega_{\rm p}^1 a_1^\dagger a_0 {\rm e}^{{\rm i}\Delta_{\rm p}^1 t} + \hbar\Omega_{\rm p}^2 a_2^\dagger a_0 {\rm e}^{{\rm i}\Delta_{\rm p}^2 t} + {\rm h.c.}, \quad (3)$$

where, a is the electron operator, and the Rabi frequency $\Omega_{\rm d(p)}^j = d_{0j}\varepsilon_{\rm d(p)}/\hbar$ with $\varepsilon_{\rm d(p)}$ being the field amplitude.

Phonon effect will be an important factor which influences the quantum transport behaviour of a CTQD system. Experiments have demonstrated that spontaneous emission of phonons dominates the nonlinear electron transport of a double QD system at mK temperature.[19] The decay rate of excited levels due to spontaneous emission of phonons can be written as follows:[20]

$$\Gamma_{ij} = 2\pi g \left(\frac{T_{\rm c}}{\Delta E_{ij}}\right)^2 \frac{\Delta E_{ij}}{\hbar} \left[1 - \frac{\sin(\Delta E_{ij}/\hbar\omega_{\rm s})}{\Delta E_{ij}/\hbar\omega_{\rm s}}\right] \times {\rm e}^{-\Delta E_{ij}/\hbar\omega_{\rm c}}, \quad (4)$$

where $\omega_{\rm s} = c_{\rm s}/d$, $c_{\rm s}$ and d are the longitudinal speed of sound and the distance between the neighboring dot centres respectively, $g \approx 0.05$ is the dimensionless coupling constant, $\Delta E_{ij} = E_j - E_i$ is the energy difference between the upper level and the lower one. Following Ref. [20], we take the exponential cutoff energy $\hbar\omega_{\rm c} = 1$ meV in the calculation.

For the studied three-level CTQD interacting with the two fields $F_{\rm d}$ and $F_{\rm p}$, electron reservoirs and phonon environment, the evolution of electron states can be described by the Liouville equation:[18,21]

$$\frac{\partial\boldsymbol{\rho}(t)}{\partial t} = -\frac{\rm i}{\hbar}[H_{\rm I}, \boldsymbol{\rho}(t)] + \Gamma_{\rm phonon}\boldsymbol{\rho}(t) + \Gamma_{\rm lead}\boldsymbol{\rho}(t), \quad (5)$$

where $\boldsymbol{\rho}(t) = |\Psi(t)\rangle\langle\Psi(t)|$ is the density matrix. The first term on the right-hand side of Eq. (5) is a reversible part describing the electron–field interaction. And the second and third terms are irreversible parts which describe the effects of the spontaneous emission of phonons and the tunneling between the CTQD and its reservoirs, respectively. By numerically calculating Eq. (5), the population probability P_i of state $|i\rangle$ can be obtained. Then, the stationary photon-assisted tunneling current is calculated from the following formula:

$$I = e[\Gamma_{\rm d}^1 P_1 + \Gamma_{\rm d}^2 P_2 - \Gamma_{\rm d}^0 P_{\rm E}]_{\rm stat} = e\Gamma_{\rm s}[P_{\rm E}]_{\rm stat}, \quad (6)$$

for the V-type CTQD or

$$I = e[\Gamma_{\rm d}^1 P_1 + \Gamma_{\rm d}^2 P_2 + \Gamma_{\rm d}^0 P_0]_{\rm stat} = e[\Gamma_{\rm s}^1 P_{\rm E} + \Gamma_{\rm s}^2 P_{\rm E} - \Gamma_{\rm s}^0 P_0]_{\rm stat}, \quad (7)$$

for the Λ-type one, where $P_{\rm E} = 1 - P_0 - P_1 - P_2$, the population probability of 'empty' state where there exists no tunneling electron in the CTQD.

2.2. Dressed states and absorption spectrum

The quantum coherent behaviour of the field-driven three-level system can be understood better from a dressed-electron picture: a fully quantised description for the electron and its driving field. The fully quantised Hamiltonian is written as

$$H^{\rm d} = \sum_{i=0}^{2} E_i a_i^\dagger a_i + \hbar\omega_{\rm d} b^\dagger b + \hbar(\kappa a_1^\dagger a_0 b + \kappa^* a_0^\dagger a_1 b^\dagger) + \hbar(\kappa a_2^\dagger a_0 b + \kappa^* a_0^\dagger a_2 b^\dagger), \quad (8)$$

where b is the photon operator, and κ is the complex coupling constant. The above Hamiltonian is further written as a sum of two terms as follows:

$$\begin{aligned} H^{\rm d} &= H_0^{\rm d} + H_{\rm I}^{\rm d}, \\ H_0^{\rm d} &= \hbar\omega_{\rm d}(a_1^\dagger a_1 + a_2^\dagger a_2 + b^\dagger b), \\ H_{\rm I}^{\rm d} &= \hbar(\omega_{10} - \omega_{\rm d}) a_1^\dagger a_1 + \hbar(\omega_{20} - \omega_{\rm d}) a_2^\dagger a_2 \\ &\quad + \hbar(\kappa a_1^\dagger a_0 b + \kappa^* a_0^\dagger a_1 b^\dagger) \\ &\quad + \hbar(\kappa a_2^\dagger a_0 b + \kappa^* a_0^\dagger a_2 b^\dagger). \end{aligned} \quad (9)$$

Using eigenstates of $H_0^{\rm d}$: $|0, n+1\rangle$, $|1, n\rangle$ and $|2, n\rangle$ with n being the photon number, as a basis, one can numerically diagonalizing the interaction Hamiltonian $H_{\rm I}^{\rm d}$ and then obtain the dressed-electron states

$$|i, n\rangle = c_{i0}|0, n+1\rangle + c_{i1}|1, n\rangle + c_{i2}|2, n\rangle \quad (10)$$

with energy E_{in} $(i = \alpha, \beta, \gamma)$.

In the dressed-electron picture, positions of the probed absorption peaks are determined by the energy intervals $E_{j,n} - E_{i,n-1}$, and the peak intensities can be calculated from the following formula:

$$\mathcal{J}(\omega_{ij}) \propto W_{ij}[\Pi_j(+\infty) - \Pi_i(+\infty)], \quad (11)$$

where, W_{ij} is the transition rate for $|i, n-1\rangle \to |j, n\rangle$, $\Pi_i(+\infty)$ and $\Pi_j(+\infty)$ are the occupation probabilities for steady-states $|i, n-1\rangle$ and $|j, n\rangle$, respectively. W_{ij} can be calculated from

$$\begin{aligned} W_{ij} &= |\langle i, n-1|\boldsymbol{e}\cdot\boldsymbol{r}|j, n\rangle|^2 \\ &= (c_{i0}c_{j1}d_{01} + c_{i0}c_{j2}d_{02})^2. \end{aligned} \quad (12)$$

The occupation probability Π_i (Π_j) can be obtained from $\boldsymbol{\rho}(t) = |\Psi(t)\rangle\langle\Psi(t)|$ through a unitary transformation $\Pi(t) = \boldsymbol{\sigma}\boldsymbol{\rho}(t)\boldsymbol{\sigma}^\dagger$, where $\boldsymbol{\sigma}$ is the transformation matrix from the bare-state basis to the dressed-state one.

3. Results and discussion

The Autler–Townes (AT) doublet and Mollow triplet are typical quantum coherent characteristics of a strongly driven three-level quantum system. For a V-type or Λ-type three-level system where one of the two transitions is coherently driven by a strong field, the weak probe absorption from the other transition splits into two resonances, known as the AT doublet splitting. When the probe absorption is on the strongly driven transition, the spectrum shows Mollow triplet splitting. Recently, these quantum interference phenomena extensively studied in atomic systems were observed in a single semiconductor QD.[15] Using the fine-structure splitting of exciton states in the QD, a V-type three-level configuration is formed consisting of two exciton states with an energy interval of 15 μeV and the crystal ground state. The two linearly polarised transitions are driven by two optical fields, and the Autler–Townes and Mollow splittings are observed in the absorption spectrum. In contrast to a single QD, a V- or Λ-type three-level configuration with adjustable energy intervals can be designed using a CTQD. Abundant quantum interference phenomena are expected in such a three-level CTQD, and can be observed not only in optical spectrum but also in spectra of photon-assisted currents.

3.1. Spectra of photon-assisted currents

We study the quantum coherent behaviour of strongly driven V-type and Λ-type CTQDs by investigating the spectra of their photon-assisted currents. The driving field $F_{\rm d}$ is set to be resonant with one of the two transitions of the three-level CTQD. By scanning the frequency of a weak probe field $F_{\rm p}$, the spectra of photon-assisted currents are obtained for various CTQDs with a varying energy interval S. In Figs. 2(a) and 2(b), we plot the photon-assisted currents of V-type and Λ-type CTQDs as functions of $\omega_{\rm p} - \omega_{0i}$ $(i = 1, 2)$ and S. The spectra of V-type and Λ-type CTQDs show similar characteristics. As the energy interval $|S|$ is large, the spectra consist of only two peaks. With $|S|$ decreasing, more peaks appear in the spectra and the peak intensities also change accordingly, and the background current increases sharply in the meanwhile. As $|S|$ decreases further and approaches zero, all peaks disappear rapidly. To see the variations of the spectra in more detail, we extract several spectrum lines from Fig. 2(a) and plot them in Fig. 3(a). At $S = -0.4$ meV, only two

peaks, with an interval of $2\Omega_{\rm d}$ and approximatively equal height, appear near $\omega_{\rm p} = \omega_{02}$. Obviously, they correspond to the well-known AT doublet. We label them with A_1 and A_2. With $|S|$ decreasing, another pair of AT doublet peaks, labeled with A_3 and A_4, can be shown at about $\omega_{\rm p} = 2\omega_{\rm d} - \omega_{02}$. Between the two pairs of AT doublet peaks, three peaks labeled with M_1, M_2 and M_3 are also seen simultaneously. The middle one M_1 lies at the resonant frequency $\omega_{\rm p} = \omega_{\rm d} = \omega_{01}$ and the two others have an interval of $2\Omega_{\rm d}$ away from M_1. They belong to the so-called Mollow triplet. We see that the spectra of photon-assisted currents exhibit the properties of absorption spectra of a three-level quantum system. A remarkable property of the spectra is that the peak intensity is very sensitive to the level structure of CTQD when $|S|$ is small. In Fig. 3(b), we plot the dependences of intensities of peak A_{1-4} with respect to their background currents on S. It can be seen that the intensities of A_1, A_3 and A_4 firstly increase and then decrease with $|S|$ decreasing, and the intensity of A_2 decreases all the while. As S is close to 0, all peaks disappear due to the symmetrical three-level configuration of the CTQD. In contrast to the AT doublet peaks, the Mollow ones always have very weak strengths. Moreover, there is a vibration near the M_1 peak (see Fig. 3(c)), and consequently part of the spectrum curve is bellow the background current. This is a near-resonant 'gain' effect which was observed recently in the absorption spectrum of a single dot.[15]

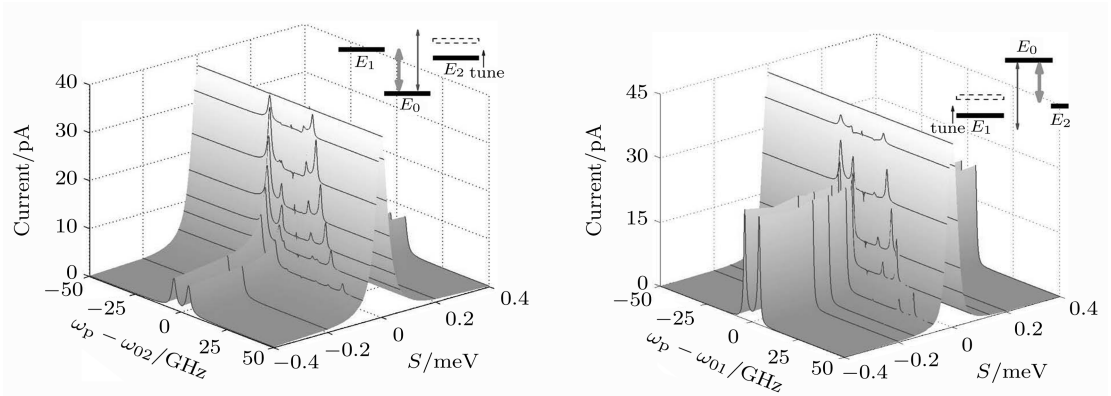


Fig. 2. (a) Photon-assisted currents of a V-type CTQD driven by a driving field $F_{\rm d}$ resonantly coupling with transition $|0\rangle \rightarrow |1\rangle$ while varying the level E_2 of $|2\rangle$ and scanning the probe field $F_{\rm p}$. The currents are plotted as functions of $S = E_2 - E_1$ and $\omega_{\rm p} - \omega_{02}$. (b) Photon-assisted currents of a Λ-type CTQD driven by $F_{\rm d}$ resonantly coupling with transition $|0\rangle \rightarrow |2\rangle$ while varying the level E_1 of $|1\rangle$ and scanning $F_{\rm p}$, as functions of S and $\omega_{\rm p} - \omega_{01}$. The relevant parameters are frequency $\omega_{\rm d} = 363$ GHz and Rabi frequency $\Omega_{\rm d} = 4$ GHz for $F_{\rm d}$, Rabi frequency $\Omega_{\rm p} = 0.5$ GHz for $F_{\rm p}$, tunneling rate $\Gamma_{\rm s} = \Gamma_{\rm d} = 1$ GHz, and the decay rate Γ_{01} (Γ_{02}) calculated from Eq. (4).

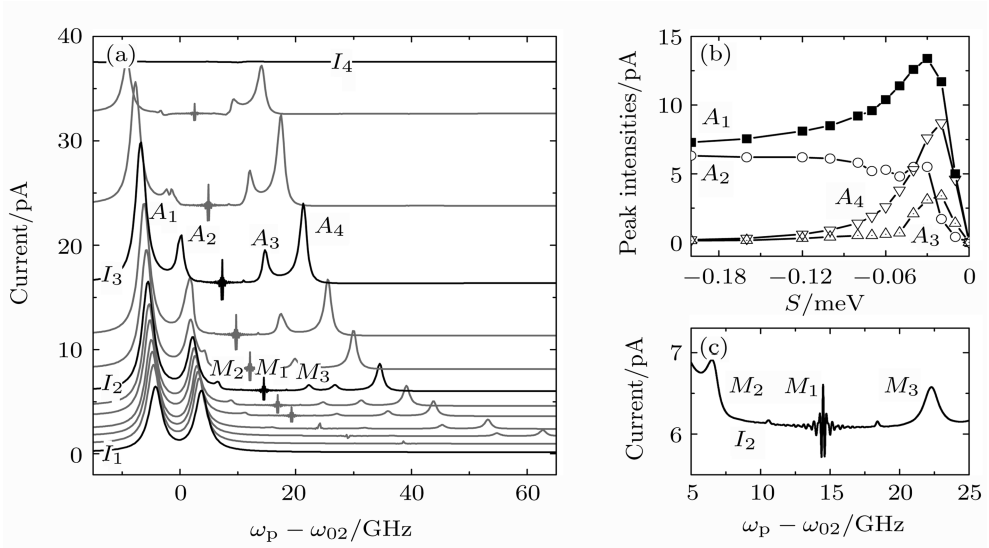


Fig. 3. (a) Current spectrum lines extracted from Fig. 2(a). The spectrum lines of $S = -0.40, -0.06, -0.03$ and 0.003 meV are marked as I_{1-4}. (b) Intensities of AT doublet peaks A_{1-4} with respect to their background currents as functions of S. (c) Mollow triplet peaks M_{1-3} in the spectrum line of $S = -0.06$ meV.

3.2. Underlying quantum coherent behaviours

To reveal the underlying quantum physics of the above spectra of CTQDs, we should investigate the absorption spectra of the three-level CTQDs under a dressed-electron picture. In Fig. 4(a), we give the variation of dressed states with S for the V-type CTQD and its driving field $F_{\rm d}$ resonantly coupling with transition $|0\rangle \rightarrow |1\rangle$. Under the action of $F_{\rm d}$, the 'bare' states $|0, n+1\rangle$, $|1, n\rangle$ and $|2, n\rangle$ become the 'dressed' states $|\alpha, n\rangle$, $|\beta, n\rangle$ and $|\gamma, n\rangle$, where n denotes the photon number of $F_{\rm d}$. They are the linear combinations of the bare states (see Eq. (10)). In Figs. 4(b)–4(d), we plot the evolutions of the components of dressed states with S. As $|S|$ is large, $F_{\rm d}$ mainly couples $|0, n+1\rangle$ and $|1, n\rangle$, and produces dressed states $|\gamma, n\rangle$ and $|\beta, n\rangle$ as bonding and anti-bonding states, respectively.

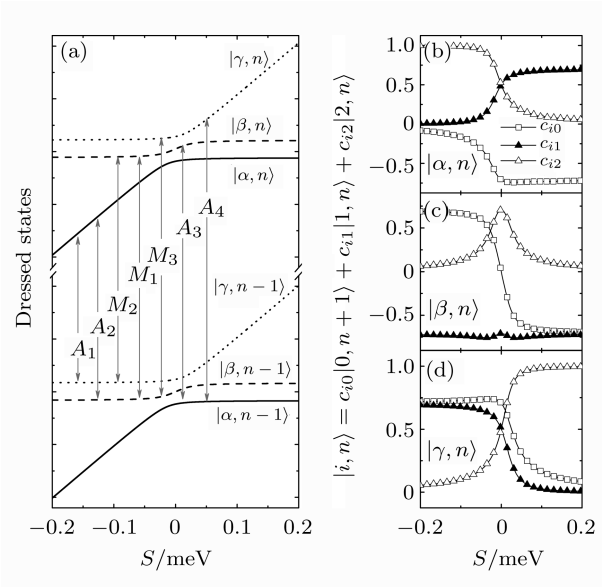


Fig. 4. (a) Dressed-electron states of the V-type CTQD and its driving field $F_{\rm d}$ for the same condition as in Figs. 2(a); (b), (c) and (d) variations of components of dressed states $|\alpha, n\rangle$, $|\beta, n\rangle$ and $|\gamma, n\rangle$, respectively.

Due to the large detuning $\Delta_{\rm d}^2$, the dressed state $|\alpha, n\rangle$ mainly consists of $|2, n\rangle$. With the decrease of $|S|$, $\Delta_{\rm d}^2$ reduces and the field $F_{\rm d}$ can couple all the three bare states. Then each dressed state includes three bare states with non-zero probabilities ρ_i $(i = 0, 1, 2)$. At $S = 0$, the three-level configuration is symmetric, and then both $|1\rangle$ and $|2\rangle$ are resonantly coupled with $|0\rangle$ by $F_{\rm d}$. A coherent superposition of the bare states occurs. The dressed states $|\alpha, n\rangle$ and $|\gamma, n\rangle$ become anti-bonding and bonding states, respectively. And the dressed state $|\beta, n\rangle$ becomes another anti-bonding state only consisting of $|1, n\rangle$ and $|2, n\rangle$, including no $|0, n+1\rangle$. It is the well-known trapping state which can lead to the absorption cancelation. In the following discussion, we will see that some interesting quantum interferences just come from the formation of such a trapping state.

The absorption peaks in spectrum correspond to transitions between dressed states: $|i, n-1\rangle \rightarrow |j, n\rangle$ $(i, j = \alpha, \beta, \gamma)$. The peak positions are determined by the energy intervals $E_{j,n} - E_{i,n-1}$. And the peak intensity is proportional to the transition rate W_{ij} and the difference of occupation probability $(\Pi_j - \Pi_i)$ (see Eq. (11)). From Eq. (12) we can see that a non-zero W_{ij} requires the initial state to include component $|0\rangle$ and the final one to include component $|1\rangle$ or $|2\rangle$ or both of them. For a three-level system, there are possible transitions with seven frequencies. In Fig. 5(a), we give the dependences of transition rates between the dressed states of the CTQD on the energy interval S. As $S < -0.1$ meV, both $W_{\alpha\beta}$ and $W_{\alpha\gamma}$, corresponding to transitions of AT doublet peaks A_3 and A_4, respectively, have near-zero values. From Fig. 4(b), we see that the initial state $|\alpha, n-1\rangle$ of the two transitions includes little component of $|0, n\rangle$ when $S < -0.1$ meV. This leads to small $W_{\alpha\beta}$ and $W_{\alpha\gamma}$. A noticeable thing is that $W_{\alpha\beta}$, $W_{\beta\alpha}$, $W_{\gamma\beta}$ and $W_{\beta\gamma}$ tend to be zero as S approaches to zero. This is an interesting quantum coherent effect resulting from the trapping state $|\beta, n-1\rangle$ $(|\beta, n\rangle)$, the initial (final) state of the four transitions. When $|\beta, n-1\rangle$ acts as an initial state of a transition, it cannot provide component $|0, n\rangle$, while $|\beta, n\rangle$ acting as a final state provides inverse coefficients $c_{\beta 1}$ and $c_{\beta 2}$. Both cases result in zero transition rates. Then, transitions between the trapping state and any other one are forbidden, and therefore, the trapping state is also called dark state. In Fig. 5(b), the occupation probabilities for dressed states are plotted as functions of S. As $|S|$ is large, electron mainly occupy $|\beta\rangle$ and $|\gamma\rangle$. With $|S|$ decreasing, occupation of $|\alpha\rangle$ increases due to the enhancement of coupling between $|0\rangle$ and $|2\rangle$. At $S = 0$, symmetrical states $|\alpha, n\rangle$ and $|\gamma, n\rangle$ have equal occupation rates Π_α and Π_γ. Figure 5(c) shows the variation of $\Delta\Pi_{ij} = \Pi_j - \Pi_i$ with S. We see that $\Delta\Pi_{\alpha\gamma}$ and $\Delta\Pi_{\beta\gamma}$ have maximum values at a certain S. $\Delta\Pi_{ii} = \Pi_i(n) - \Pi_i(n-1) = 0$ $(i = \alpha, \beta, \gamma)$ means that $|i, n\rangle$ and $|i, n-1\rangle$ are equally populated. Here a first order approximation is adopted when the number of photons, n, in field $F_{\rm d}$ has a dispersion Δn around the mean value $\overline{n}$ which is large in absolute value, small in relative value: $1 \ll \Delta n \ll \overline{n}$.[22]

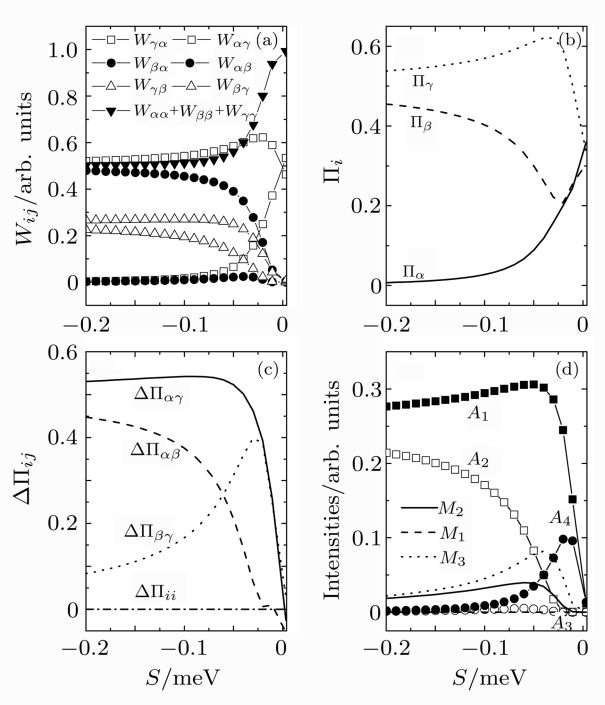


Fig. 5. Transition rates between dressed states (a). Occupation probabilities (b) and their differences (c) of dressed states. Intensities of AT doublet A_{1-4} and Mollow triplet M_{1-3} in absorption spectrum (d).

With W_{ij} and $\Delta\Pi_{ij}$, the intensities of peaks in absorption spectra can be obtained (see Eq. (11)) as shown in Fig. 5(d). There exist maximum intensities for $A_{1,3,4}$ and $M_{2,3}$. And the dependences of intensities of A_{1-4} and $M_{2,3}$ on S are similar to those in the spectra of photon-assisted currents. All the peaks vanish at $S = 0$, but there are two different reasons for their such behaviours. For $A_{1,4}$, it is because of $\Pi_\alpha = \Pi_\gamma$, while for $A_{2,3}$ and $M_{2,3}$, it is because of their zero-value transition rates $W_{i\beta}$ ($W_{\beta i}$). Of course, absorption peak M_1 always has a zero intensity because $|i, n-1\rangle$ and $|i, n\rangle$ are equally populated ($\Delta\Pi_{ii} = 0$). However, in the spectra of photon-assisted currents of CTQDs, M_1 has a vibrating intensity, showing a 'gain' effect. It comes from the coherently exchanging interaction between the driving and probe fields and does not correspond to population inversion.[15] Another noticeable result is that intensities of $M_{2,3}$ are stronger than those of A_3 in Fig. 5(d), but they are weaker than those of A_3 in the spectra of photon-assisted current spectra in Fig. 3(a). In fact, only when a transition induced by an optical absorbtion obviously enhances the population on state $|2\rangle$ of the V-type CTQD, can it demonstrate itself in the photon-assisted current. The transitions of $M_{2,3}$ occur mainly between $|0\rangle$ and $|1\rangle$ and hardly change the population on $|2\rangle$, which leads to their weaker intensities in the spectra of photon-assisted currents. On a whole, the spectrum of photon-assisted current of the CTQD still exhibits the properties of quantum coherent absorption.

3.3. Phonon effect

The electron behaviour of a CTQD always manifests itself in its phonon environment. Therefore, the phonon effect can strongly affect the spectrum of the CTQD, in particular, as it is comparable to the effect of the optical field. At low temperature, the main effect of phonon is the spontaneous emission of phonons which leads to decay of excited electron. Using Eq. (4) and according to the related experiment, we calculate the decay rate Γ_{ij} between the two states $|i\rangle$ and $|j\rangle$ of the two adjacent dots as a function of the energy difference $\Delta E_{ij} = E_j - E_i$ as shown in Fig. 6(a). In

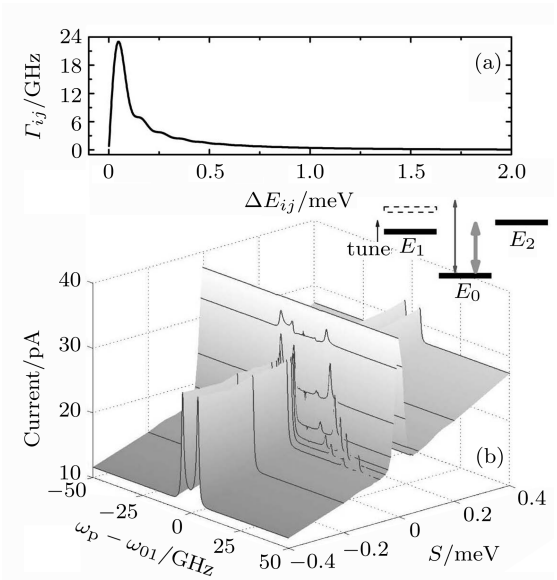


Fig. 6. (a) Decay rate as a function of energy difference $\Delta E_{ij} = E_i - E_j$ between two neighbouring dot states $|i\rangle$ and $|j\rangle$, with taking $\hbar\omega_s = 15.7$ μeV. (b) Photon-assisted currents of V-type CTQD by changing E_1 and scanning ω_p of F_p, with the field F_d resonantly coupling at transition $|0\rangle \rightarrow |2\rangle$ at $\omega_{02} = 363$ GHz, and the other parameters being the as same as those in Fig. 2(a).

our study, corresponding to the variation of the energy difference ΔE_{01} (ΔE_{02}), Γ_{01} (Γ_{02}) changes from 0.66 to 0.30 GHz. The Rabi frequency of the probe field F_p is $\Omega_p = 0.5$ GHz, comparable to Γ_{01} (Γ_{02}), while that of the driving field F_d is $\Omega_d = 4$ GHz, far larger than Γ_{01} (Γ_{02}). For the V-type CTQD, the phonon spontaneous emission Γ_{01} helps the electron tunneling transport, while Γ_{02} holds it back. If F_d couples states $|0\rangle$ and $|2\rangle$, it can eliminate the disadvantage

of Γ_{02}. Then the phonon-assistant current caused by Γ_{01} appears as a large background current as shown in Fig. 6(b). On the contrary, if $F_{\rm d}$ couples $|0\rangle$ and $|1\rangle$, the weak $F_{\rm p}$ cannot eliminate the disadvantage of Γ_{02}, then the background current is small as seen in Fig. 2(a). Similar effects can also occur in a Λ-type CTQD. By using these phonon-assistant current phenomena, which transition is driven by the strong field can be determined in experiment.

4. Conclusions

We study the photon-assisted current spectra of CTQDs driven by a strong and a weak field. Using the ground states of the three QDs, the optically coupled levels are designed as V-type or Λ-type three-level configuration. Quantum interference phenomena are revealed in the probe absorption spectra of the field-driven CTQD. When the eigenfrequency difference $\Delta\omega$ between the two pairs of transitions, formed between the middle and the left (right) dots, is large, there is one Autler–Townes splitting in probe spectrum. With the decrease of $\Delta\omega$, the strong driving field can couple the two transitions simultaneously and two Autler-Townes splittings and one weak Mollow triplet are observed in one spectrum line. As $\Delta\omega = 0$, corresponding to a completely symmetric CTQD, a large tunneling current is induced due to the effect of coherent trapping, and no absorption peaks can be observed in the spectrum. We also investigate the effect of phonon spontaneous emission on the current spectra, and reveal that the intensity of phonon-assistant background current depends on which transition is driven by the strong field.

References

[1] Waugh F R, Berry M J, Mar D J, Westervelt R M, Campman K L and Gossard A C 1995 *Phys. Rev. Lett.* **75** 705

[2] Schröer D, Greentree A D, Gaudreau L, Eberl K, Hollenberg L C L, Kotthaus J P and Ludwig S 2007 *Phys. Rev.* B **76** 075306

[3] Rogge M C and Haug R J 2008 *Phys. Rev.* B **77** 193306

[4] Ladrón de Guevara M L and Orellana P A 2006 *Phys. Rev.* B **73** 205303

[5] Xie W, Chu W D, Zhang W and Duan S Q 2008 *J. Phys.*: *Condens. Matter* **20** 325223

[6] Duan S Q, Zhang W, Xie W, Ma Y and Chu W D 2009 *New J. Phys.* **11** 013037

[7] Žitko R and Bonča J 2007 *Phys. Rev. Lett.* **98** 047203

[8] Kuzmenko T, Kikoin K and Avishai Y 2004 *Phys. Rev.* B **69** 195109

[9] Saraga D S and Loss D 2003 *Phys. Rev. Lett.* **90** 166803

[10] Kim J, Melnikov D V, Leburton J P, Austing D G and Tarucha S 2006 *Phys. Rev.* B **74** 035307

[11] Delgado F, Shim Y P, Korkusinski M and Hawrylak P 2007 *Phys. Rev.* B **76** 115332

[12] Liu B C, Pan X Q, Tian Q and Wu Z L 2006 *Chin. Phys.* **15** 1067

[13] Zhu B H, Wang F F, Zhang K, Ma G H, Gu Y Z, Guo L J and Qian S X 2008 *Acta Phys. Sin.* **57** 6557 (in Chinese)

[14] Dong Q R 2008 *Chin. Phys.* B **17** 1400

[15] Xu X, Sun B, Berman P R, Steel D G, Bracker A S, Gammon D and Sham L J 2007 *Science* **317** 929

[16] Wingreen N S, Jacobsen K W and Wilkins J W 1989 *Phys. Rev.* B **40** 11834

[17] Kwapiński T, Taranko R and Taranko E 2005 *Phys. Rev.* B **72** 125312

[18] Brandes T and Renzoni F 2000 *Phys. Rev. Lett.* **85** 4148

[19] Fujisawa T, Oosterkamp T H, van der Wiel W G, Broer BW, Aguado R, Tarucha S and Kouwenhoven L P 1998 *Science* **282** 932

[20] Brandes T and Kramer B 1999 *Phys. Rev. Lett.* **83** 3021

[21] Narducci L M, Scully M O, Oppo G L, Ru P and Tredicce J R 1990 *Phys. Rev.* A **42** 1630

[22] Cohen-Tannoudji C and Reynaud S 1977 *J. Phys.* B: *Atom. Molec. Phys.* **10** 345